STATE OF THE CLIMATE IN 2021

THE TROPICS

H. J. Diamond and C. J. Schreck, Eds.

Special Online Supplement to the *Bulletin of the American Meteorological Society*, Vol.103, No. 8, August 2022

https://doi.org/10.1175/BAMS-D-22-0069.1.

Corresponding author: Howard J. Diamond / howard.diamond@noaa.gov

STATE OF THE CLIMATE IN 2021
The Tropics

Editors
Jessica Blunden
Tim Boyer

Chapter Editors

Freya Aldred
Peter Bissolli
Kyle R. Clem
Howard J. Diamond
Matthew L. Druckenmiller
Robert J. H. Dunn
Catherine Ganter
Nadine Gobron
Gregory C. Johnson
Rick Lumpkin
Ademe Mekonnen
John B. Miller
Twila A. Moon
Marilyn N. Raphael
Ahira Sánchez-Lugo
Carl J. Schreck III
Richard L. Thoman
Kate M. Willett
Zhiwei Zhu

Technical Editor

Laura Ohlmann

BAMS Special Editor for Climate

Michael A. Alexander

American Meteorological Society

Cover credit:
Hurricane Ida hits near the Louisiana and Mississippi border on August 29, 2021 bringing high winds, flooding and a dangerous storm surge as seen. © Warren Faidley, Getty

The Tropics is one chapter from the *State of the Climate in 2021* annual report and is available from https://doi.org/10.1175/BAMS-D-22-0069.1. Compiled by NOAA's National Centers for Environmental Information, *State of the Climate in 2021* is based on contributions from scientists from around the world. It provides a detailed update on global climate indicators, notable weather events, and other data collected by environmental monitoring stations and instruments located on land, water, ice, and in space. The full report is available from https://doi.org/10.1175/2022BAMSStateoftheClimate.1.

How to cite this document:

Citing the complete report:
Blunden, J. and T. Boyer, Eds., 2022: State of the Climate in 2021. *Bull. Amer. Meteor. Soc.,* **103** (8), Si–S465, https://doi.org/10.1175/2022BAMSStateoftheClimate.1.

Citing this chapter:
Diamond, H.J. and C. J. Schreck, Eds., 2022: The Tropics [in "State of the Climate in 2021"]. *Bull. Amer. Meteor. Soc.,* **103** (8), S193–S256, https://doi.org/10.1175/BAMS-D-22-0069.1.

Citing a section (example):
Halpert, M. S., M. L'Heureux, A. Kumar, E. Becker, and Z.-Z. Hu, 2022: ENSO and the tropical Pacific [in "State of the Climate in 2021"]. *Bull. Amer. Meteor. Soc.,* **103** (8), S199–S203, https://doi.org/10.1175/BAMS-D-22-0069.1.

Editor and Author Affiliations (alphabetical by name)

Allgood, Adam, NOAA/NWS Climate Prediction Center, College Park, Maryland
Becker, Emily J., University of Miami Rosenstiel School of Marine and Atmospheric Science, Miami, Florida
Blake, Eric S., NOAA/NWS National Hurricane Center, Miami, Florida
Bringas, Francis G., NOAA/OAR/AOML Physical Oceanography Division, Miami, Florida
Camargo, Suzana J., Lamont-Doherty Earth Observatory, Columbia University, Palisades, New York
Chen, Lin, Institute for Climate and Application Research (ICAR)/KLME/ILCEC/CIC-FEMD, Nanjing University of Information Science and Technology, Nanjing, China
Coelho, Caio A. S., CPTEC/INPE Center for Weather Forecasts and Climate Studies, National Institute for Space Research, Cachoeira Paulista, Brazil
Diamond, Howard J., NOAA/OAR Air Resources Laboratory, College Park, Maryland
Fauchereau, Nicolas, National Institute of Water and Atmospheric Research, Ltd., Auckland, New Zealand
Goldenberg, Stanley B., NOAA/OAR/AOML Hurricane Research Division, Miami, Florida
Goni, Gustavo, NOAA/OAR/AOML Physical Oceanography Division, Miami, Florida
Halpert, Michael S., NOAA/NWS Climate Prediction Center, College Park, Maryland
He, Qiong, Earth System Modeling Center, Nanjing University of Information Science and Technology, Nanjing, China
Hu, Zeng-Zhen, NOAA/NWS Climate Prediction Center, College Park, Maryland
Klotzbach, Philip J., Department of Atmospheric Science, Colorado State University, Fort Collins, Colorado
Knaff, John A., NOAA/NESDIS Center for Satellite Applications and Research, Fort Collins, Colorado
Kumar, Arun, NOAA/NWS Climate Prediction Center, College Park, Maryland
Landsea, Chris W., NOAA/NWS National Hurricane Center, Miami, Florida
L'Heureux, Michelle, NOAA/NWS Climate Prediction Center, College Park, Maryland
Lin, I.-I., National Taiwan University, Taipei, Taiwan
Lorrey, Andrew M., National Institute of Water and Atmospheric Research, Ltd., Auckland, New Zealand
Luo, Jing-Jia, Institute for Climate and Application Research (ICAR)/KLME/ILCEC/CIC-FEMD, Nanjing University of Information Science and Technology, Nanjing, China
Magee, Andrew D., Centre for Water, Climate and Land, School of Environmental and Life Sciences, University of Newcastle, Callaghan, NSW, Australia
Pasch, Richard J., NOAA/NWS National Hurricane Center, Miami, Florida
Pezza, Alexandre B., Greater Wellington Regional Council, Wellington, New Zealand
Rosencrans, Matthew, NOAA/NWS Climate Prediction Center, College Park, Maryland
Schreck III, Carl J., North Carolina State University, North Carolina Institute for Climate Studies, Cooperative Institute for Satellite Earth System Studies, Asheville, North Carolina
Trewin, Blair C., Australian Bureau of Meteorology, Melbourne, Victoria, Australia
Truchelut, Ryan E., WeatherTiger LLC, Tallahassee, Florida
Wang, Bin, SOEST, Department of Meteorology and IPRC, University of Hawaii, Honolulu, Hawaii
Wang, Hui, NOAA/NWS Climate Prediction Center, College Park, Maryland
Wood, Kimberly M., Department of Geosciences, Mississippi State University, Mississippi State, Mississippi
Woolley, John-Mark, National Institute of Water and Atmospheric Research, Ltd., Auckland, New Zealand

Editorial and Production Team

Allen, Jessicca, Graphics Support, Cooperative Institute for Satellite Earth System Studies, North Carolina State University, Asheville, North Carolina
Hammer, Gregory, Content Team Lead, Communications and Outreach, NOAA/NESDIS National Centers for Environmental Information, Asheville, North Carolina
Love-Brotak, S. Elizabeth, Lead Graphics Production, NOAA/NESDIS National Centers for Environmental Information, Asheville, North Carolina
Misch, Deborah J., Graphics Support, Innovative Consulting and Management Services, LLC, NOAA/NESDIS National Centers for Environmental Information, Asheville, North Carolina
Ohlmann, Laura, Technical Editor, Innovative Consulting and Management Services, LLC, NOAA/NESDIS National Centers for Environmental Information, Asheville, North Carolina
Riddle, Deborah B., Graphics Support, NOAA/NESDIS National Centers for Environmental Information, Asheville, North Carolina
Veasey, Sara W., Visual Communications Team Lead, Communications and Outreach, NOAA/NESDIS National Centers for Environmental Information, Asheville, North Carolina

4. Table of Contents

*Please refer to Chapter 8 (Relevant datasets and sources) for a list of all climate variables and datasets used in this chapter for analyses, along with their websites for more information and access to the data.

Severe Tropical Cyclone Niran, the third severe TC and second Category 5 TC for the season, initially formed off the coast of northern Queensland and was named on 1 March (see section 4g7) while tracking towards the southwest. Niran intensified to a Category 5 system on 5 March on approach to New Caledonia, achieving peak 10-minute sustained winds of 110 kt (57 m s^{-1}) and a minimum central pressure of 931 hPa. Unfavorable wind shear weakened the system to a Category 3 event before it passed close to the southern coastline of New Caledonia.

h. Tropical cyclone heat potential—F. Bringas, G. J. Goni, I-I Lin, and J. A. Knaff

Tropical cyclone heat potential (TCHP; e.g., Goni et al. 2009, 2017) is an indicator of the available heat stored in the upper ocean that can potentially induce tropical cyclone (TC) intensification and regulate ocean–atmosphere enthalpy fluxes and TC-induced sea surface temperature (SST) cooling (e.g., Lin et al. 2013). TCHP is calculated as the integrated heat content between the sea surface and the 26°C isotherm (D26), which is generally taken to be the minimum temperature required for TC genesis and intensification (Leipper and Volgenau 1972; Dare and McBride 2011).

Provided that atmospheric conditions are favorable, TC intensification, including rapid intensification, has been associated with areas in the ocean that have TCHP values above 50 kJ cm^{-2} (e.g., Shay et al. 2000; Mainelli et al. 2008; Lin et al. 2014; 2021; Knaff et al. 2018, 2020). High SSTs prior to TC formation usually lead to less SST cooling during the lifetime of the TC, and hence higher enthalpy fluxes from the ocean into the storm, favoring intensification (e.g., Lin et al. 2013). Similarly, upper ocean salinity is another condition of relevance for TC intensification because fresh water-induced barrier layers may also modulate the upper ocean mixing and cooling during a TC, and hence the air–sea fluxes (e.g., Balaguru 2012; Domingues et al. 2015). Upper ocean thermal conditions observed during 2021 are presented here in terms of two parameters: (1) TCHP anomaly values with respect to their long-term mean (1993–2020) and (2) TCHP anomaly values compared to conditions observed in 2020. TCHP anomalies during 2021 (Fig. 4.40) are computed for June–November in the Northern Hemisphere and November 2020–April 2021 in the Southern Hemisphere. In Fig. 4.40, the seven regions where TCs are known to form, travel, and intensify are highlighted. In all of these regions, TCHP values exhibit large temporal and spatial variability due to mesoscale features, trends, and short- to long-term modes of variability, such as the North Atlantic Oscillation (NAO), El Niño-Southern Oscillation (ENSO), and the Pacific Decadal Oscillation (PDO). The differences in TCHP anomalies between 2020 and 2021 are also computed for the primary months of TC activity in each hemisphere (Fig. 4.41).

During the 2021 season, TCHP exhibited above-average values across most basins (Fig. 4.40). TCHP anomalies above 30 kJ cm^{-2} were observed in areas within several regions, including the North Indian Ocean, southeast Indian Ocean, western Pacific Ocean, and the Gulf of Mexico. These positive anomalies may be indicative of favorable oceanic conditions during 2021 for TC development and intensification. Compared to 2020, TCHP anomalies in 2021 were higher in the southeast Indian Ocean, southwest Pacific, and part of the Gulf of Mexico basin, while the anomalies were lower in the rest of the basins (Fig. 4.41). In particular, TCHP anomalies during 2021 were lower than those in 2020 and below the long-term average in the eastern North Pacific basin, linked to the negative phase of ENSO (La Niña) that re-emerged in August 2021.

In the Southern Hemisphere, TCHP during 2021 was mostly above the long-term average, with values of more than 30 kJ cm^{-2} in the southeast Indian Ocean and ~10 kJ cm^{-2} in the southwest Indian Ocean (Fig. 4.40). TCHP was more than 20 kJ cm^{-2} higher than 2020 values in the southeast Indian Ocean and southwest Pacific, while they were 20 kJ cm^{-2} lower in areas of the southwest Indian Ocean (Fig. 4.41). The 2020/21 cyclone season in the southwest Indian Ocean was above average and produced seven TCs of Category 1 or above intensity, including Very Intense TC Faraji (Category 5; section 4g6). Ocean conditions with high TCHP anomalies in the southeast Indian Ocean and southwest Pacific around Australia translated, however, to a below-average but deadly season with five TCs, including Severe TC Seroja and Category 5 Niran (section 4g8), the most

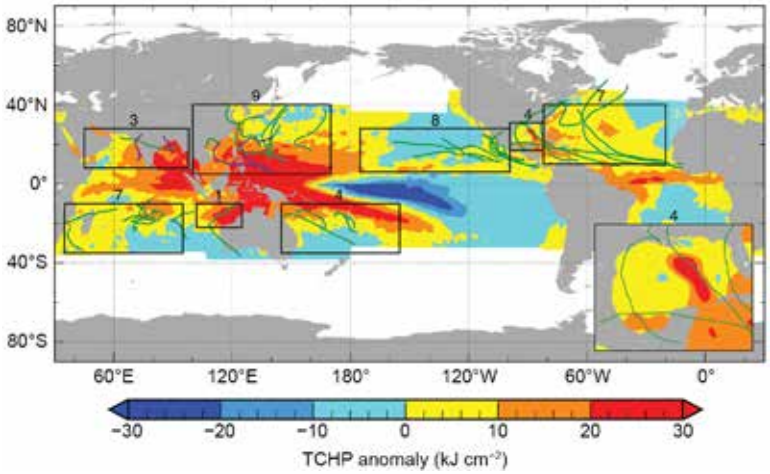

Fig. 4.40. Global anomalies of TCHP (kJ cm^{-2}) during 2021 computed as described in the text. The boxes indicate the seven regions where TCs occur: from left to right, southwest Indian, North Indian, northwest Pacific, southeast Indian, South Pacific, East Pacific, and North Atlantic (shown as Gulf of Mexico and tropical Atlantic separately). The green lines indicate the trajectories of all tropical cyclones reaching at least Category 1 (1-min average wind ≥ 64 kt, 34 m s^{-1}) and above during Nov 2020–Apr 2021 in the Southern Hemisphere and Jun–Nov 2021 in the Northern Hemisphere. The purple lines indicate the trajectories of tropical cyclones Category 1 or stronger in the Northern Hemisphere that occurred outside the Jun–Nov 2021 period. The numbers above each box correspond to the number of Category 1 and stronger cyclones that travel within each box. The Gulf of Mexico conditions are shown in the inset in the lower right corner.

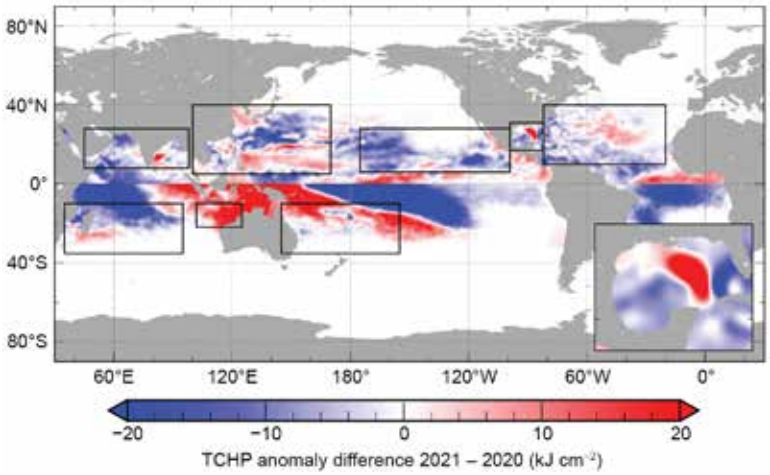

Fig. 4.41. TCHP anomaly difference (kJ cm^{-2}) between the 2021 and 2020 tropical cyclone seasons (Jun–Nov in the Northern Hemisphere and Nov–Apr in the Southern Hemisphere). The Gulf of Mexico conditions are shown in the inset in the lower right corner.

intense storm of the region for this season. Anomalously high values of TCHP in the Coral Sea were partially responsible for Niran's slow, but steady, development just off the coast of Queensland while being nearly stationary and noticeably affected by vertical wind shear on 2–3 March, followed by its rapid intensification that commenced once the storm began to move on 4 March.

The North Indian Ocean was characterized by above-average TCHP during 2021, with anomalies in excess of 30 kJ cm^{-2} in the Bay of Bengal (Fig. 4.40); however, these values were lower than those observed the previous year (Fig. 4.41). Three Category 1 or stronger TCs occurred in the region (Fig. 4.40), two of which occurred in May and are shown in Fig. 4.40 as purple lines. The most intense TC in this basin during 2021 was Extremely Severe TC Tauktae in May (section 4g5), with peak intensity of 3-minute sustained wind speed of 100 kt (51 m s^{-1}) and minimum pressure of 950 hPa. TCHP values exceeding 140 kJ cm^{-2} over the southeast Arabian Sea were cited as a contributing environmental factor, noting values were lower but exceeding 50 kJ cm^{-2} along the storm track (IMD 2021).

Upper ocean thermal conditions are largely modulated by the state of ENSO in the North Pacific (e.g., Lin et al. 2014, 2020; Zheng et al. 2015). During 2021, La Niña was observed from August to the end of the year. This is similar to 2020, in which a stronger La Niña (compared to 2021) was observed during August 2020 to May 2021. As is typical during a La Niña year, TCHP was above average in the western North Pacific (Lin et al. 2014, 2020), with anomalies well above 30 kJ cm^{-2} closer to the equator and average anomalies of ~20 kJ cm^{-2} throughout the region compared to the long-term average (Fig. 4.40). Compared to 2020, TCHP in the western North Pacific displayed both negative and positive anomalies, possibly associated with the difference in the La Niña characteristics of these two years. TCHP anomalies were slightly negative compared to average in the eastern North Pacific and moderately negative compared to 2020 (Fig. 4.41). Category 5 Super Typhoon Surigae was the most intense storm both in the western North Pacific and globally in 2021. Interestingly, it occurred

in April (i.e., boreal spring) and not summer and is therefore shown in Fig. 4.40 as a purple track line. TCHP observations show that Surigae intensified to 165 kts (85 m s^{-1}) peak intensity over a region of high TCHP of ~120–140 kJ cm^{-2}, ~30 kJ cm^{-2} higher than the long-term mean for April. Another notable western North Pacific Category 5 TC was Super Typhoon Chanthu, which intensified to its peak intensity of 155 kts (80 m s^{-1}) in September, when traveling over the Kuroshio warm current region south of Taiwan, where high TCHP values of ~130 kJ cm^{-2} were observed.

In the North Atlantic basin, upper ocean thermal conditions during the 2021 hurricane season were characterized by TCHP values moderately above the long-term average, with anomalies between +10 and +20 kJ cm^{-2} (Fig. 4.40) but as much as 10 kJ cm^{-2} lower than the previous year in the regions where most TCs form and intensify in this basin (Fig. 4.41). An exception was the area associated with the location of the northern extension of the Loop Current in the Gulf of Mexico, where TCHP anomalies were more than 30 kJ cm^{-2} higher than the long-term average and more than 20 kJ cm^{-2} higher than the values of 2020. Consistent with the higher-than-average TCHP anomalies, 2021 was the third most active Atlantic hurricane season on record with 21 named storms, including seven hurricanes at Category 1 or above intensity.

During 2021, Hurricanes Grace and Ida reached their peak intensities, corresponding to Category 3 and 4 storms, respectively. The genesis of Hurricane Grace started off Cabo Verde on 10 August. The system continued to organize and became a named tropical storm on 14 August, reaching Category 1 when traveling in the Caribbean Sea. After the storm moved offshore from the Yucatan Peninsula into the southwest region of the Gulf of Mexico, Grace underwent rapid intensification on 23 August from Category 1 to Category 3 in a 15-hour period while moving over an area with SST > 28°C and TCHP > 60 kJ cm^{-2}, above the 50-kJ cm^{-2} threshold required to support Atlantic hurricane intensification (Mainelli et al. 2008). Hurricane Ida, the second most intense Atlantic storm in 2021, reached Category 1 when traveling on 26–27 August over an area in the Caribbean Sea with favorable ocean conditions, including TCHP values of more than 120 kJ cm^{-2} and extensive areas of low salinity surface layers associated with the Amazon and Orinoco riverine plumes, observed by underwater gliders deployed in the region (https://www.aoml.noaa.gov/hurricane-glider-project). Low-surface salinity areas create barrier layer conditions that reduce upper-ocean turbulent mixing and maintain high enthalpy fluxes from the ocean into the hurricane, therefore contributing to TC organization and intensification (e.g., Balaguru et al. 2015; Domingues et al. 2015). After traveling over the western portion of Cuba and entering the Gulf of Mexico, Ida moved over a region of increasingly favorable ocean conditions over the main location of the northern extension of the Loop Current, the same area where the largest TCHP anomalies in the North Atlantic and Gulf of Mexico basins occurred (Fig. 4.40). These favorable conditions contributed to Ida's intensification, including rapid intensification reaching Category 4 on 29 August with peak intensity of 1-minute sustained wind speeds of 130 kt (67 m s^{-1}) and a minimum central barometric pressure of 929 hPa, after traveling over a warm region with TCHP > 140 kJ cm^{-2} associated with a strong anticyclonic eddy that was shed by the Loop Current.

In summary, favorable upper-ocean thermal conditions were observed in all seven basins during the 2021 season, except in the eastern North Pacific, where conditions were average to slightly below average compared to the long-term mean. Additionally, TCHP anomaly values during 2021 exhibited similar to lower values in most regions compared to the previous year in most basins.